

See discussions, stats, and author profiles for this publication at: <https://www.researchgate.net/publication/325474311>

Nonlinear Model Order Reduction of Thermoelectric Generator for Electrically Active Implants

Conference Paper · May 2018

CITATIONS

0

READS

102

1 author:



[Onkar Sandip Jadhav](#)

Technische Universität Berlin

4 PUBLICATIONS 4 CITATIONS

SEE PROFILE

Some of the authors of this publication are also working on these related projects:



Model order reduction for parametric high dimensional models in the analysis of financial Risk [View project](#)

Nonlinear Model Order Reduction of Thermoelectric Generator for Electrically Active Implants.

O.S. Jadhav¹, C.D. Yuan^{1,2}, E. Rudnyi³, D. Hohlfeld¹, T. Bechtold^{1,2}

¹Institute of Electronic Appliances and Circuits, University of Rostock, Rostock, Germany

²Department of Engineering, Jade University of Applied Sciences, Wilhelmshaven, Germany

³CADFEM GmbH, Germany

Introduction

An ever increasing aging of the European population necessitates the development of different medical treatments for regenerative therapies. Self-powered electrically active implants help the electrical stimulation of body tissue to accelerate its regeneration. Deep brain stimulation has proven to be effective in treating movement disorders like Parkinson's disease and dystonia. One of the major drawbacks of current implants is their limited lifetime. This results into risky and expensive surgeries to replace the depleted unit. Harvesting of mechanical or thermal body energy and converting it into electrical power creates a pathway to improve the implants lifetime up to energy autonomy.

The human body has a core temperature of 37 °C. To maintain this temperature, body tissue generates warmth by metabolic heat generation [1]. Additionally, heat is transferred to body tissue through its perfusion by blood. In our previous work [2] we considered the effect of perfusion as a homogeneous heat generation rate.

In this work, we present a multiphysical model of a miniaturized thermoelectric generator (TEG) for electrically active implants. The device generates a voltage from temperature gradients across human tissue by the Seebeck effect. Furthermore, we combine the mathematical technique of model order reduction (MOR) with the nonlinear perfusion heat generation in order to come up with a compact but highly accurate thermal model.

Model Description

A simplified tissue model consisting of muscle, fat and skin layers, as suggested in [3] has been built. The miniaturized TEG is embedded into the fat layer (see Fig. 1), which exhibits the highest temperature gradient. The heat conduction in the tissue can be described by the bioheat equation of Pennes [4]:

$$\rho C \frac{\partial T}{\partial t} = K \frac{\partial^2 y}{\partial x^2} + Q_b + Q_m, \quad (1)$$

where, $Q_b = \rho_b C_b \omega_b (T_a - T(\vec{r}))$ and Q_m are blood perfusion and metabolic heat generation rates respectively. ρ , C , K are the density, specific heat and thermal conductivity of the muscle tissue. ρ_b , C_b denote the thermal properties of blood and ω_b is a measure of blood perfusion. $T(\vec{r})$ is the resulting temperature distribution and $T_a = 37^\circ\text{C}$, is the core body temperature. Furthermore, the heat is dissipated by convection from the skin surface with a heat transfer

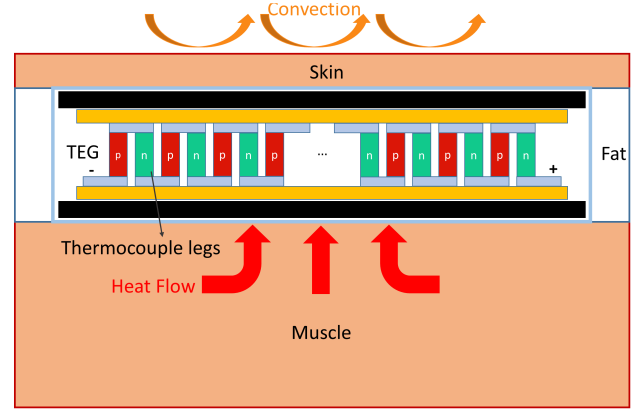


Figure 1: Schematic of a thermo-electric active implant positioned in the fat layer

coefficient of 20 W/m²K whereas the environmental temperature is set to 14.85 °C.

Model Order Reduction

By applying the Finite Element Method (FEM), the thermal model can be spatially discretized and represented as follows:

$$\sum_n \begin{cases} E \cdot \dot{T}(t) = A \cdot T(t) + B \cdot u(T(t)) \\ y(t) = C \cdot T(t), \end{cases} \quad (2)$$

where, $A, E \in R^{n \times n}$ are the global heat conductivity and heat capacity matrices, $B \in R^{n \times m}$ is the input matrix and $C \in R^{n \times p}$ is the output matrix. Here, n is the dimension of the system, m and n are the number of inputs and user defined outputs.

After applying the block-Arnoldi algorithm to the above MIMO system having n inputs and n outputs, we obtain the reduced order model as follows [5]:

$$\sum_r \begin{cases} E_r \cdot \dot{z}(t) = A_r \cdot z(t) + B_r \cdot u(z) \\ y(t) = C_r \cdot z(t), \end{cases} \quad (3)$$

where, $E_r = V^T E V$, $A_r = V^T A V$, $B_r = V^T B$, $C_r = C V$. V is a projection matrix. State space vector $T(t)$ is represented as follows:

$$T(t) = V \cdot z(t) + \varepsilon \quad (4)$$

The goal is to find V , such that the projection error ε can be neglected. The projection matrix V is constructed as an



orthonormal basis of the right Krylov-subspace which is defined as follows:

$$K_r\{P, b\} = \text{span}\{b, P^2b, \dots, P^{r-1}b\} \quad (5)$$

where we set $P = A^{-1}E$ and $b = A^{-1}B$. The reduced system (3) is the same structure as the full model (2) with dimension $r \ll N$. Most important is that, the input and output vectors u and y are preserved during the model order reduction which means the accuracy of the reduced model is guaranteed.

Nonlinear Input at System-level

In order to obtain an accurate model, we integrate the nonlinear source term within the system-level model. As illustrated above the tissue structure consists of muscle, fat and skin layers. The muscle tissue, in which the heat generation due to blood perfusion is prominent, is divided into q segments. Fig. 2 shows the muscle tissue segmented into 5 divisions. During model order reduction, we apply separate heat generation rates across the q segments. The average temperatures of each segments are defined as outputs (T_{avg}), which leads to a linear multiple input multiple output (MIMO) system. Additional temperature outputs are defined by the temperature difference across the TEG (top and bottom surface of TEG). Furthermore, we import the generated reduced order model into the system level simulator.

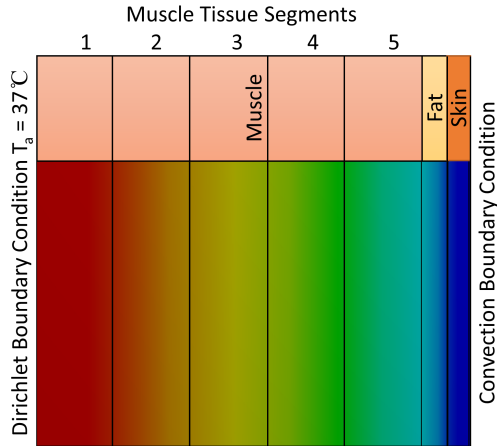


Figure 2: Muscle tissue segmented into five parts with temperature distribution across the human body tissue.

From (1), the perfusion heat generation rate is given as:

$$Q_b = \rho_b C_b \omega_b (T_a - T_{avg}) + Q_m \quad (6)$$

where, $T_a = 37^\circ\text{C}$, $Q_m = 988 \text{ W/m}^3$, $\rho_b = 1049.75 \text{ kg/m}^3$, $C_b = 3617 \text{ J/kgK}$.

As the muscle tissue is divided into q segments, we can represent the above nonlinear equation in each part of the muscle tissue as:

$$Q_i = \rho_b C_b \omega_b (T_{a_i} - T_{avg_i}) + Q_m/q, \quad i = 1, 2, \dots, q \quad (7)$$

where, T_{a_i} denotes the surface temperatures of each tissue segment and T_{avg_i} denotes the average temperature respectively.

We can consider (7) by feeding the average temperature outputs (T_{avg_i}) to the inputs (Q_i). (see Fig. 3 for a system-level model with muscle tissue segmented into 2 parts.)

Here, T_{amb} is the ambient temperature, T_a is the body core

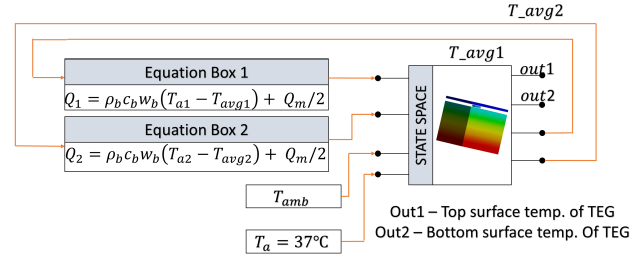


Figure 3: System-level model for implementing the nonlinear heat generation input with muscle tissue segmented into two parts.

temperature specified at the back surface of muscle tissue. $T_{a1,2}$ denotes the surface temperatures of each part of muscle tissue.

Results and Discussion

A temperature distribution obtained from a steady state simulation with a film coefficient of $20 \text{ W/m}^2\text{K}$ was considered as an initial state. Transient thermal simulations were carried out with a film coefficient of $15 \text{ W/m}^2\text{K}$ to represent changing environmental conditions. The temperature values at the top and bottom surface of the TEG have been chosen as outputs. Fig. 4 shows the temperature dis-

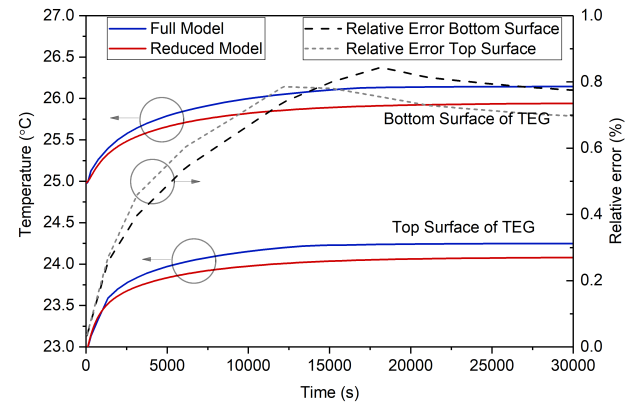


Figure 4: Temperature result comparison between the full and reduced model at the bottom and top surfaces of a TEG with muscle tissue segmented into five parts. The relative error between the full and reduced model is shown on the right axis.

tribution of the full model of order 127,648 and reduced model of order 30. A considerable difference exists between the full and the reduced model; maximum relative

error of 0.843%. To obtain more accurate results we carried out the simulation with muscle tissue divided into ten and fifteen segments.

Fig. 5 illustrates the temperature results for muscle tissue divided into ten segments. We observe that the results match with minimal error. Furthermore, we divide the mus-

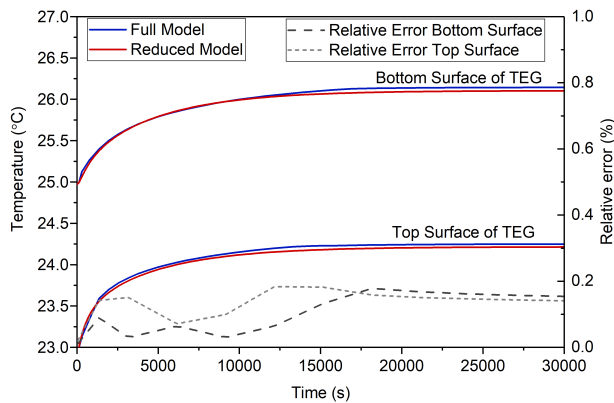


Figure 5: Temperature result of the full and the reduced model at the bottom and top surfaces of a TEG with muscle tissue divided into ten segments.

cle tissue into 15 segments. An excellent match is obtained (See Fig. 6). MOR has proven its applicability and efficiency as the computational time for the reduced model is only 17.421 s, which is several orders of magnitude smaller compared to the full model which takes 1550 s for the simulation.

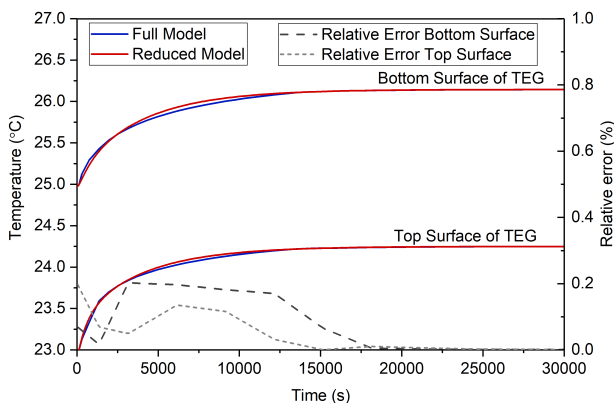


Figure 6: Temperature result for the full and reduced model at the bottom and top surfaces of a TEG with muscle tissue divided into fifteen segments.

Conclusion

In this work, we presented the results of transient thermal simulation of a TEG within human tissue and the methodology of considering the non-linear heat generation due to blood perfusion. The non-linearity was considered at the system-level. Furthermore, it was shown that with increas-

ing number of muscle tissue segments, the accuracy of the model increases as well.

References

- [1] Ken Parsons. *Human thermal environments*. CRC Press Inc, 3 edition, 2014.
- [2] Onkar Jadhav, Cheng Dong Yuan, Dennis Hohlfeld, and Tamara Bechtold. Design of a thermoelectric generator for electrical active implants. *MikroSystemTechnik congress 2017*, page 3.1, 2017.
- [3] Yang Yang, Xiao-Juan Wei, and Jing Liu. Suitability of a thermoelectric power generator for implantable medical electronic devices. *Journal of Physics D: Applied Physics*, 40(18):5790–5800, 2007.
- [4] H. H. Pennes. Analysis of tissue and arterial blood temperatures in the resting human forearm. *Journal of Applied Physiology*, 85(1):5–34, 1998.
- [5] Roland W. Freund. Krylov-subspace methods for reduced-order modeling in circuit simulation. *Journal of Computational and Applied Mathematics*, 123(1-2):395–421, 2000.